

Chemically Authentic Surrogate Mixture Model for the Thermophysical Properties of a Coal-Derived Liquid Fuel

M. L. Huber, E. W. Lemmon, V. Diky, B. L. Smith, and T. J. Bruno*

Physical and Chemical Properties Division, National Institute of Standards and Technology (NIST),
Boulder, Colorado 80305

Received May 5, 2008. Revised Manuscript Received June 11, 2008

We developed a surrogate mixture model to represent the physical properties of a coal-derived liquid fuel using only information obtained from a gas chromatography–mass spectrometry analysis of the fuel and a recently developed “advanced distillation curve”. We then predicted the density, speed of sound, and viscosity of the fuel and compared them to limited experimental data. The surrogate contains five components (*n*-propylcyclohexane, *trans*-decalin, α -methyldecalin, bicyclohexane, and *n*-hexadecane), yet comparisons to limited experimental data demonstrate that the model is able to represent the density, sound speed, and viscosity to within 1, 4, and 5%, respectively.

Introduction

Recently, there has been renewed interest in synthetic liquid fuels derived from natural gas, coal, or biomass feedstocks. Lamprecht¹ discussed the use of Fischer–Tropsch fuels by the U.S. military. Feedstocks derived from coal (coal-derived fuel or CDF) are of particular interest because there are large domestic supplies of coal. Engine designers and manufacturers require reliable information on the thermophysical properties of these new fuels to optimize the design process. In this work, we will provide thermophysical property models for a blended fuel made from a significant fraction of coal liquids that is referred to as prototype JP-900.

Because these fuels are usually complex mixtures of many hydrocarbon species, a surrogate model approach is often the best approach to model these fuels. Edwards and Maurice² reviewed some of the surrogates available for aviation and rocket fuels and provided an overview of the general requirements and expectations of fuel surrogates.

Several research groups have proposed surrogate fuel mixtures for gasoline, diesel fuel, and aviation turbine fuel. These proposed mixtures, which number in the dozens, vary in complexity, and most are intended for specific purposes. Single-component surrogates may be adequate for simple applications. More complex, multicomponent surrogate mixtures are required for measurements and studies that are dependent upon fuel chemistry. Examples of such applications include soot formation, emissions, radiation loading, combustion staging, or applications involving lean premixed flames. Surrogate mixtures are also relevant to the study of physical properties. Specifically, the properties that describe fuel volatility (distillation properties, vapor pressures, etc.) are needed for the study of preferential vaporization phenomena and pool fire hazards.

Previously, we used a surrogate model approach to model the thermophysical properties of a synthetic aviation fuel derived

from natural gas.³ In this work, we implemented a similar procedure to develop a surrogate model for a synthetic aviation fuel derived from coal. Here, however, we used only information from a distillation curve measurement and a chemical analysis to develop the surrogate model. Then, we compared how well this model, derived from only these two experimental inputs, can represent the density, sound speed, and viscosity of an actual fuel. In contrast to previous work,^{3,4} the mixture model that we have developed here is predictive in the sense that we did not use density, sound speed, or viscosity measurements to develop the surrogate model.

The procedure for developing a surrogate mixture for the coal-derived fluid can be summarized as follows. First, a chemical analysis was performed to identify the composition of the fuel sample. From this analysis, a list of representative fluids was constructed, including compounds representative of the various chemical families (branched or straight-chain alkanes, alkenes, aromatics, naphthenes, etc.) found in the sample. For each of these possible pure-fluid constituents, an equation of state and a viscosity surface were needed. To represent the thermophysical properties of a mixture, mixture models were used that incorporate the pure fluid equations for both thermodynamic and transport properties. The fluids in the surrogate mixture and their compositions were found by determining the composition that minimized the difference between the predicted and experimental distillation curve for the fuel sample. One could include additional constraints, such as C/H ratio, but in this work, we used only the distillation curve.

The fuel sample that we modeled in this work was obtained from the Air Force Research Laboratory Propulsion Directorate (AFRL, Wright Patterson Air Force Base, Dayton, OH). This sample was designated POSF-4765, and its ultimate source was the Pennsylvania State University Energy Institute's Coal

*To whom correspondence should be addressed. E-mail: bruno@boulder.nist.gov.

(1) Lamprecht, D. Fischer–Tropsch fuel for use by the U.S. military as battlefield-use fuel of the future. *Energy Fuels* **2007**, *21* (3), 1448–1453.

(2) Edwards, T.; Maurice, L. Q. Surrogate mixtures to represent complex aviation and rocket fuels. *J. Propul. Power* **2001**, *17* (2), 461–466.

(3) Huber, M. L.; Smith, B. L.; Ott, L. S.; Bruno, T. J. Surrogate mixture model for the thermophysical properties of synthetic aviation fuel S-8: Explicit application of the advanced distillation curve. *Energy Fuels* **2008**, *22*, 1104–1114.

(4) Magee, J. W.; Bruno, T. J.; Friend, D. G.; Huber, M. L.; Laesecke, A.; Lemmon, E. W.; McLinden, M. O.; Perkins, R. A.; Baranski, J.; Widgren, J. A. *Thermophysical Properties Measurements and Models for Rocket Propellant RP-1: Phase I*; NIST: Boulder, CO, 2007.

Table 1. Potential Constituent Fluids for the Surrogate Fuel Mixture

compound	CAS number	number of carbon atoms	boiling point at 83 kPa (K)	normal boiling point (K)
methylcyclohexane	108-87-2	7	367.1	374.0
<i>n</i> -propylcyclohexane	1678-92-8	9	422.1	429.9
<i>trans</i> -decalin	493-02-7	10	451.9	460.3
<i>cis</i> -decalin	493-01-6	10	460.4	468.9
α -methyldecalin (isomer not specified)	2958-75-0	11	471.1	479.9
2,6-dimethyldecalin	1618-22-0	12	472.0	480.9
<i>n</i> -hexylcyclohexane	4292-75-5	12	489.6	498.2
bicyclohexyl	92-51-3	12	502.1	511.1
<i>n</i> -hexadecane	544-76-3	16	551.0	560.1

Utilization Laboratory. In an earlier paper,⁵ we reported the analysis of the sample by gas chromatography and mass spectrometry and found 31 major constituents ranging from cyclohexane to eicosane. The predominant species were cyclic compounds of 10–12 carbons, especially decalins. From this analysis, we formulated a list of nine representative compounds to be used for the development of the surrogate; these are listed in Table 1 along with their normal boiling points and their boiling points at an atmospheric pressure of 83 kPa (the typical local pressure of our laboratory). For each monobranched decalin identified in the chemical analysis,⁵ a representative species was selected as a candidate constituent fluid for the surrogate. In other words, for our purposes all *x*-methyldecalins are represented as a single methyldecalin. Similarly, we used a particular *x,y*-dimethyl decalin to represent the dimethyldecalin family. We did not consider positional isomers except for *cis*- and *trans*-decalin. A major factor governing the specific choice of compound to represent a moiety was the availability of property data: priority was given to compounds for which the most abundant and reliable experimental measurements were available. After this procedure, for each possible constituent fluid, we searched the open literature as well as databases, such as NIST TDE,⁶ DIPPR,⁷ and Landolt–Bornstein⁸ for experimental physical property data. For some of the fluids, the data are limited and were supplemented with predicted values.

Properties of the Constituent Pure Fluids

Because our modeling approach³ requires thermophysical property models for all pure constituent fluids, it was necessary to develop equations of state for the potential constituent pure fluids. We used mixtures of real components, similar to the method suggested by Eckert and Vanek,⁹ instead of pseudo-components, as is common in the petroleum industry. Two of the candidate fluids, methyl and *n*-propyl cyclohexane, have been studied in previous work,^{10–12} and thermodynamic and

transport surfaces are available. For the other fluids, it was necessary to develop new property surfaces. To facilitate this task, we used the ThermoData Engine program,⁶ described by Diky et al.¹³ that provides dynamic data evaluation and on-demand generation of equation-of-state parameters. We selected the Span–Wagner equation of state,¹⁴ which can represent well not only the vapor pressure and density but also other properties, such as the speed of sound and heat capacity. In contrast to a simple cubic equation of state, such as the Peng–Robinson EOS,¹⁵ which requires only minimal information (critical temperature and pressure, acentric factor) the Helmholtz form (an equation of state explicit in Helmholtz energy as a function of density and temperature) requires experimental data to determine the multiple parameters of the equation. For fluids with extremely limited experimental data (such as those with only a normal boiling point and a liquid density), the TDE program⁶ provides predictive data for properties to supplement the experimental data. Although other equations of state can be used, such as a generalized Helmholtz form¹⁶ that requires only the critical point and the acentric factor, or a volume-translated¹⁷ form of the original Peng–Robinson EOS,¹⁵ we preferred the Span–Wagner form because it allows the flexibility to fit whatever limited data are available and it can represent all thermodynamic properties well.

The Span–Wagner equation of state is formulated in terms of the molar Helmholtz free energy as a function of density and temperature

$$a(\rho, T) = a^0(\rho, T) + a^r(\rho, T) \quad (1)$$

where a is the molar Helmholtz energy, $a^0(\rho, T)$ is the ideal gas contribution to the molar Helmholtz energy, and $a^r(\rho, T)$ is the real fluid molar Helmholtz energy that results from intermolecular forces. All thermodynamic properties can be calculated as derivatives of the Helmholtz energy.¹⁴ In practical applica-

(5) Smith, B. L.; Bruno, T. J. Composition-explicit distillation curves of aviation fuel JP-8 and a coal-based jet fuel. *Energy Fuels* **2007**, *21* (5), 2853–2862.

(6) Frenkel, M.; Chirico, R. D.; Diky, V.; Muzny, C.; Lemmon, E. W.; Yan, X.; Dong, Q. *NIST Standard Reference Database 103, NIST ThermoData Engine: Version 3.0, Standard Reference Data*; National Institute of Standards and Technology: Gaithersburg, MD, 2008.

(7) Rowley, J. R.; Wilding, W. V.; Oscarson, J. L.; Rowley, R. L. *DIADDEM, DIPPR Information and Data Evaluation Manager, 2.0*; Brigham Young University: Provo, UT, 2002.

(8) Wohlfarth, C.; Wohlfarth, B. *Viscosity of Pure Organic Liquids and Binary Liquid Mixtures*; Landolt–Bornstein–Numerical Data and Function Relationships in Science and Technology, IV/18; Springer-Verlag: Berlin, Germany, 2001; Vol. subvolume B. Pure Organic Liquids.

(9) Eckert, E.; Vanek, T. Extended utilization of the characterization of petroleum mixtures based on real components. *Chem. Pap.* **2005**, *59* (6A), 428–433.

(10) Laesecke, A.; Outcalt, S. L.; Brumback, K. Density and speed of sound measurements of methyl- and propylcyclohexane. *Energy Fuels* **2008**, manuscript submitted.

(11) Bruno, T. J. The properties of S-8 and JP-10. Report prepared for Wright Laboratory Aero Propulsion Power Directorate under MIPR F4FBEY6346G001, 2007.

(12) Perkins, R. A.; Hammerschmidt, U.; Huber, M. L. Measurement and correlation of the thermal conductivity of methylcyclohexane and propylcyclohexane from 300 to 600 K at pressures to 60 MPa. *J. Chem. Eng. Data* **2008**, manuscript submitted.

(13) Diky, V.; Muzny, C. D.; Lemmon, E. W.; Chirico, R. D.; Frenkel, M. ThermoData Engine (TDE): Software implementation of the dynamic data evaluation concept. 2. Equations of state on demand and dynamic updates over the web. *J. Chem. Inf. Model.* **2007**, *47*, 1713–1725.

(14) Span, R.; Wagner, W. Equations of state for technical applications. I. Simultaneously optimized functional forms for nonpolar and polar fluids. *Int. J. Thermophys.* **2003**, *24* (1), 1–39.

(15) Peng, D.; Robinson, D. B. New 2-constant equation of state. *Ind. Eng. Chem. Fundam.* **1976**, *15* (1), 59–64.

(16) Xiang, H. W.; Deiters, U. K. A new generalized corresponding-states equation of state for the extension of Lee–Kesler equation to fluids consisting of polar and larger nonpolar molecules. *Chem. Eng. Sci.* **2008**, *63* (6), 1490–1496.

(17) Peneloux, A.; Rauzy, E.; Freze, R. A consistent correction for Redlich–Kwong–Soave volumes. *Fluid Phase Equilib.* **1982**, *8* (1), 7–23.

tions, the functional form used is the dimensionless Helmholtz energy, α , as a function of a dimensionless density and temperature. The form of this equation is

$$\frac{a(\rho, T)}{RT} = \alpha(\delta, \tau) = \alpha^0(\delta, \tau) + \alpha^r(\delta, \tau) \quad (2)$$

where $\delta = \rho/\rho_c$ and $\tau = T/T_c$. The Helmholtz energy of the ideal gas is given by

$$a^0 = h_0^0 + \int_{T_0}^T c_p^0 dT - RT - T \left[s_0^0 + \int_{T_0}^T \frac{c_p^0}{T} dT - R \ln \left(\frac{\rho T}{\rho_0 T_0} \right) \right] \quad (3)$$

where ρ_0 is the ideal-gas density at T_0 and p_0 ($\rho_0 = p_0/T_0 R$). The values of T_0 , p_0 , h_0^0 , and s_0^0 are arbitrary and can be chosen based on user's desired reference values of enthalpy and entropy. The ideal gas Helmholtz energy is given in a dimensionless form by

$$\alpha^0 = \frac{h_0^0 \tau}{RT_c} - \frac{s_0^0}{R} - 1 + \ln \frac{\delta \tau_0}{\delta_0 \tau} - \frac{\tau}{R} \int_{\tau_0}^{\tau} \frac{c_p^0}{\tau^2} d\tau + \frac{1}{R} \int_{\tau_0}^{\tau} \frac{c_p^0}{\tau} d\tau \quad (4)$$

where $\delta_0 = \rho_0/\rho_c$ and $\tau_0 = T_0/T_c$.

The calculation of thermodynamic properties from the ideal-gas Helmholtz energy requires an equation for the ideal gas heat capacity, c_p^0 . The TDE⁶ program provides the ability to generate formulations for the ideal-gas heat capacity by use of several different functional forms. Values for the ideal-gas heat capacity were estimated by use of the method of Joback and Reid¹⁸ with group parameters re-evaluated at NIST/TRC¹⁹ and then fit to the following form used in reference equations of state^{20,21} that is expressed in terms of "Planck–Einstein" functions:

$$c_p^0 = c_0 T^{c_1} + c_2 \frac{(c_3/T)^2 \exp(c_3/T)}{[1 - \exp(c_3/T)]^2} + c_4 \frac{(c_5/T)^2 \exp(c_5/T)}{[1 - \exp(c_5/T)]^2} + c_6 \frac{(c_7/T)^2 \exp(c_7/T)}{[1 - \exp(c_7/T)]^2} \quad (5)$$

In eq 5, the temperature is in K and c_p^0 is in J mol⁻¹ K⁻¹. The coefficients for the Planck–Einstein equation were obtained with a nonlinear least-squares algorithm by use of the simplex method. Further details on the regression methods in the TDE program can be found in ref 13. This form of equation can extrapolate reliably to high temperatures that may be of interest in fuel applications and is superior to common polynomial fits that often have unphysical behavior when extrapolated beyond the range over which they were fitted.

The functional form used for the residual Helmholtz energy equation of state for a pure fluid is

$$\alpha^r(\delta, \tau) = \sum_{k=1}^{N_t} n_k \delta^{i_k} \tau^{j_k} + \sum_{k=1}^{N_t} n_k \delta^{i_k} \tau^{j_k} \exp(-\delta^{i_k}) \quad (6)$$

where the summation is over the N_t total terms of the equation. The form used in this work, developed by Span and Wagner,¹⁴

(18) Joback, K. G.; Reid, R. C. Estimation of pure-component properties from group contributions. *Chem. Eng. Commun.* **1987**, *57*, 233–243.

(19) Frenkel, M.; Chirico, R. D.; Diky, V.; Yan, X. J.; Dong, Q.; Muzny, C. ThermoData Engine (TDE): Software implementation of the dynamic data evaluation concept. *J. Chem. Inf. Model.* **2005**, *45* (4), 816–838.

(20) Wagner, W.; Pruss, A. The IAPWS formulation 1995 for the thermodynamic properties of ordinary water substance for general and scientific use. *J. Phys. Chem. Ref. Data* **2002**, *31* (2), 387–535.

(21) Lemmon, E. W.; Jacobsen, R. T. A new functional form and new fitting techniques for equations of state with application to pentafluoroethane (HFC-125). *J. Phys. Chem. Ref. Data* **2005**, *34* (1), 69–108.

has 12 terms. The coefficients in this equation are obtained by simultaneously fitting experimental data for multiple properties (for example, vapor pressure, density, sound speed, and heat capacity).

For viscosity, we used models capable of representing the entire fluid surface rather than limited range correlations. Poling et al.²² discuss several options. Dependent upon the fluid, the viscosity was modeled with either an extended corresponding states model^{22,23} or a variation of the model of Chung et al.^{22,24} Both models can be used in a predictive mode when data are scarce and require only the critical parameters and acentric factor ω for nonpolar fluids. Two additional parameters (a dimensionless dipole moment μ_r and an empirical correction factor for hydrogen bonding κ) are included in the Chung et al. model to account for polarity and hydrogen bonding. In both models, the dilute gas is represented with the Chapman–Enskog theory²⁵ along with the empirical correlation of Neufeld et al.²⁶ for the collision integrals. Chung et al.²⁴ present relations for the potential parameters ϵ/k and σ in terms of the critical volume and the critical temperature; alternatively, the potential parameters may be estimated with a corresponding states method.²⁷

When sufficient data are available, the representation of the viscosity can be improved by fitting the data to model parameters. For the model of Chung et al.,²⁴ we retained the dilute gas parameters as presented in the original paper. However, for the dense fluid contribution, we treated all five parameters (σ^* , ϵ^*/k , ω^* , μ_r^* , and κ^*) as empirical parameters found by regressing available data. (We use the parameters in the same context as in the original model of Chung et al.²⁴ but use an asterisk to denote that we treat them as totally empirical parameters that no longer retain their original meaning.) Viscosity calculated with the extended corresponding states model described in ref 23 may also be improved by fitting data to correction functions for the shape factors that are expressed as (see eq 10 in ref 23)

$$\psi(\rho_r) = d_0 + d_1 \rho_r + d_2 \rho_r^2$$

where ψ is the correction function for the shape factors expressed as a polynomial in reduced density $\rho_r = \rho/\rho_c$ and the coefficients d_0 , d_1 , and d_2 are constants found from fitting the experimental viscosity data. Dodecane was used as a reference fluid because it is similar to the constituent fluids and has formulations available for both the equilibrium²⁸ and transport properties.²⁹

The equations of state and ideal gas heat capacity formulations were developed with the TDE program⁶ with methods described in ref 13. The formulations for the viscosity surface were obtained by fitting experimental data or using predictive

(22) Poling, B. E.; Prausnitz, J. M.; O'Connell, J. P. *The Properties of Gases and Liquids*, 5th ed.; McGraw-Hill: New York, 2001.

(23) Huber, M. L.; Laesecke, A.; Perkins, R. A. Model for the viscosity and thermal conductivity of refrigerants, including a new correlation for the viscosity of R134a. *Ind. Eng. Chem. Res.* **2003**, *42* (13), 3163–3178.

(24) Chung, T. H.; Ajlan, M.; Lee, L. L.; Starling, K. E. Generalized multiparameter correlation for nonpolar and polar fluid transport properties. *Ind. Eng. Chem. Res.* **1988**, *27* (4), 671–679.

(25) Chapman, S.; Cowling, T. G. *The Mathematical Theory of Non-uniform Gases*; Cambridge University Press: Cambridge, U.K., 1952.

(26) Neufeld, P. D.; Janzen, A. R.; Aziz, R. A. Empirical equations to calculate 16 of the transport collision integrals $\Omega^{(L,S)}$ for the Lennard–Jones (12–6) potential. *J. Chem. Phys.* **1972**, *57* (3), 1100–1102.

(27) Huber, M. L.; Ely, J. F. Prediction of the viscosity of refrigerants and refrigerant mixtures. *Fluid Phase Equilib.* **1992**, *80*, 239–248.

(28) Lemmon, E. W.; Huber, M. L. Thermodynamic properties of n-dodecane. *Energy Fuels* **2004**, *18* (4), 960–967.

(29) Huber, M. L.; Laesecke, A.; Perkins, R. Transport properties of n-dodecane. *Energy Fuels* **2004**, *18* (4), 968–975.

Table 2. Fluid-Specific Parameters

(a) <i>n</i> -Hexadecane				
critical parameters	T_c (K)	p_c (kPa)	ρ_c (mol/L)	
	722.4	1459.0	0.9965	
c_p^0 parameters	c_0	c_1	c_2	c_3
	34.0588	0.321249	247.482	1745.74
	c_4	c_5	c_6	c_7
	225.029	3036.43	242.095	795.502
EOS parameters				
k	n_k	i_k	j_k	l_k
1	1.70163173911	0.32	1	0
2	−3.25180919862	1.23	1	0
3	0.299104359531	1.5	1	0
4	−0.215427393737	1.4	2	0
5	0.0927951193067	0.07	3	0
6	$3.23908982507 \times 10^{-4}$	0.8	7	0
7	1.14486118331	2.16	2	1
8	0.0766349207708	1.1	5	1
9	−0.58582491551	4.1	1	2
10	−0.14393490805	5.6	4	2
11	0.0119536613035	14.5	3	3
12	0.00402626369301	12	4	3
ECS parameters for viscosity				
d_0	d_1	d_2		
1.03257	4.21494×10^{-3}	-4.93431×10^{-3}		
(b) <i>cis</i> -Decalin				
critical parameters	T_c (K)	p_c (kPa)	ρ_c (mol/L)	
	702.14	3067.8	2.061	
c_p^0 parameters	c_0	c_1	c_2	c_3
	16.2006	0.04987	227.639	1560.19
	c_4	c_5	c_6	c_7
	172.759	629.775	265.069	3155.14
EOS parameters				
k	n_k	i_k	j_k	l_k
1	1.18777583272	0.25	1	0
2	−3.41875329754	1.125	1	0
3	1.47715942129	1.5	1	0
4	−0.172685192181	1.375	2	0
5	0.128206310606	0.25	3	0
6	0.000263477454385	0.875	7	0
7	0.0439559205361	0.625	2	1
8	−0.0882813084332	1.75	5	1
9	−0.489747441532	3.625	1	2
10	−0.135056120113	3.625	4	2
11	0.00774955851609	14.5	3	3
12	0.00164587000053	12	4	3
viscosity parameters				
σ^*	ε^*/k	ω^*	μ_t^*	κ^*
0.748444	502.556	−0.0203294	1.02422	0.047536
(c) <i>trans</i> -Decalin				
critical parameters	T_c (K)	p_c (kPa)	ρ_c (mol/L)	
	686.95	2843.4	2.007	
c_p^0 parameters	c_0	c_1	c_2	c_3
	16.2006	0.04987	227.639	1560.19
	c_4	c_5	c_6	c_7
	172.759	629.775	265.069	3155.14

Table 2. Continued

EOS parameters				
k	n_k	i_k	j_k	l_k
1	1.2432974665	0.25	1	0
2	-2.74465872026	1.125	1	0
3	1.14341762006	1.5	1	0
4	-0.359406007682	1.375	2	0
5	0.114801573715	0.25	3	0
6	0.0003232429318	0.875	7	0
7	-0.45885857634	0.625	2	1
8	-0.0111668661998	1.75	5	1
9	-0.527821401572	3.625	1	2
10	-0.0215292177513	3.625	4	2
11	0.0429011813393	14.5	3	3
12	-0.0406366965152	12	4	3
viscosity parameters				
σ^*	ε^*/k	ω^*	μ_r^*	κ^*
0.752783	355.565	0.130383	1.17997	0.0738838
(d) Bicyclohexyl				
critical parameters	T_c (K)	p_c (kPa)	ρ_c (mol/L)	
	742.0	2751.8	1.6975	
c_p^0 parameters	c_0	c_1	c_2	c_3
	9.19418	0.414485	290.079	2952.49
	c_4	c_5	c_6	c_7
	172.844	810.024	180.4	1640.63
EOS parameters				
k	n_k	i_k	j_k	l_k
1	1.24988569761	0.25	1	0
2	-3.08211766283	1.25	1	0
3	0.183508725475	1.5	1	0
4	0.111563445247	0.25	3	0
5	0.000346686605193	0.875	7	0
6	1.16020908538	2.375	1	1
7	1.18455500055	2	2	1
8	-0.00912900438556	2.125	5	1
9	-0.714151426206	3.5	1	2
10	-0.038134795714	6.5	1	2
11	-0.17150825439	4.75	4	2
12	-0.00402009762522	12.5	2	3
viscosity parameters				
d_0	d_1			d_2
0.9424	0.034208			0.0
(e) <i>n</i> -Hexylcyclohexane				
critical parameters	T_c (K)	p_c (kPa)	ρ_c (mol/L)	
	675.0	1796.7	1.462	
c_p^0 parameters	c_0	c_1	c_2	c_3
	23.8463	0.194234	342.027	1484.84
	c_4	c_5	c_6	c_7
	146.775	435.788	202.92	3055.19
EOS parameters				
k	n_k	i_k	j_k	l_k
1	0.997734484373	0.25	1	0
2	-2.54235465337	1.125	1	0
3	0.75040916695	1.5	1	0
4	-0.53120903763	1.375	2	0
5	0.155048270441	0.25	3	0
6	0.00028878763926	0.875	7	0
7	0.96549668861	0.625	2	1
8	0.0647269523949	1.75	5	1
9	-0.829230271123	3.625	1	2
10	-0.205902056943	3.625	4	2
11	-0.0161961984139	14.5	3	3
12	0.0120541492413	12	4	3

Table 2. Continued

viscosity parameters				
d_0	d_1	d_2		
1.03	0	0		
(f) α -Methyldecalin				
critical parameters	T_c (K)	p_c (kPa)	ρ_c (mol/L)	
	697	2612.31	1.846	
c_p^0 parameters	c_0	c_1	c_2	c_3
	19.3732	0.173857	184.106	707.963
	c_4	c_5	c_6	c_7
	224.164	1608.54	278.013	3105.54
EOS parameters				
k	n_k	i_k	j_k	l_k
1	1.00816390879	0.25	1	0
2	-2.83068196679	1.125	1	0
3	0.780190804635	1.5	1	0
4	-0.174630992875	1.375	2	0
5	0.117581480067	0.25	3	0
6	0.00025291388631	0.875	7	0
7	0.674225724947	0.625	2	1
8	-0.029287601328	1.75	5	1
9	-0.490461596644	3.625	1	2
10	-0.15198792486	3.625	4	2
11	-0.0326667010223	14.5	3	3
12	0.0209990542317	12	4	3
viscosity parameters				
d_0	d_1	d_2		
1.05	0	0		
(g) 2,6-Dimethyldecalin				
parameters	T_c (K)	p_c (kPa)	ρ_c (mol/L)	ω
	690.0	2334.	1.666	0.342
c_p^0 parameters	c_0	c_1	c_2	c_3
	2.07603	0.500393	173.513	524.164
	c_4	c_5	c_6	c_7
	248.818	1394.49	313.787	2917.32
EOS parameters				
k	n_k	i_k	j_k	l_k
1	1.23187847214	0.25	1	0
2	-3.48965601431	1.125	1	0
3	1.39446873932	1.5	1	0
4	-0.182505041018	1.375	2	0
5	0.132869094418	0.25	3	0
6	0.000268480350611	0.875	7	0
7	0.218550615514	0.625	2	1
8	-0.0753516507514	1.75	5	1
9	-0.535028434641	3.625	1	2
10	-0.119708832539	3.625	4	2
11	0.0254255425933	14.5	3	3
12	-0.016862228025	12	4	3
viscosity parameters				
d_0	d_1	d_2		
1.03	0	0		

methods. The resulting coefficients for the pure fluids (except methyl and *n*-propylcyclohexane, which are in ref 11) are given in parts a–g of Table 2. The critical temperature was set to the value recommended by the TDE program,⁶ while the critical density and pressure were obtained by fitting during the development of the EOS. To estimate the reliability of these

formulations, a short description of comparisons with selected experimental data for each fluid is given below.

Bicyclohexyl. The speed of sound data^{30,31} are represented to within 2%; the saturation heat capacity data³² are within 3%; the high temperature (424–577 K) vapor pressure measurements of Wiczorek and Kobayashi³³ are within 2%; while the vapor pressure measurements of Myers and Fenske³⁴ that cover a wider range of 331–511 K show deviations as large as 8%. The density data of Chang et al.³⁵ that extend to 30 MPa at temperatures from 333 to 413 K are within 0.3%. The limited viscosity data of Evans³⁶ are represented to within 2% and cover the temperature range 278–363 K. There were limited viscosity data for this fluid, with no data at pressures above the saturation boundary; however, we estimate the uncertainty to be less than 10% in the liquid phase.

trans-Decalin. The speed of sound data^{37,38} are represented to within 1%; the heat capacity at saturation data³⁹ are represented to within 2%. Deviations in vapor pressure^{40–42} are within 2%; saturated liquid densities^{37,43,44} are within 0.2%; and density data^{43–45} as a function of pressures less than 100 MPa are within 1%. On the basis of comparisons to the data of Zeberg-Mikkelsen et al.⁴³ that cover 293–353 K at pressures to 100 MPa and the data of Seyer and Leslie,⁴⁶ we estimate the uncertainty of the viscosity in the liquid phase as 5%.

***n*-Hexadecane.** Speed of sound data of Bolotnikov et al.⁴⁷ over the range 293–373 K along the liquid saturation boundary

(30) Tardajos, G.; Pena, M. D.; Lainez, A.; Aicart, E. Speed of sound in and isothermal compressibility and isobaric expansivity of pure liquids at 298.15 K. *J. Chem. Eng. Data* **1986**, *31* (4), 492–493.

(31) Weissler, A. Ultrasonic investigation of molecular properties of liquids. 4. Cyclic compounds. *J. Am. Chem. Soc.* **1949**, *71* (2), 419–421.

(32) Chirico, R. D.; Cowell, A. B.; Good, W. D.; Klots, T. D.; Knipmeyer, S. E.; Nguyen, A.; Rau, A. P.; Reynolds, J. W.; Smith, N. K.; Steele, W. V. Heat capacities, enthalpy increments, phase transitions, and derived thermodynamic functions for the condensed phases of bicyclohexyl between the temperatures 6 and 440 K. *J. Chem. Thermodyn.* **1998**, *30* (12), 1423–1439.

(33) Wiczorek, S. A.; Kobayashi, R. Vapor-pressure measurements of diphenylmethane, thianaphthene, and bicyclohexyl at elevated temperatures. *J. Chem. Eng. Data* **1980**, *25* (4), 302–305.

(34) Myers, H. S.; Fenske, M. R. Measurement and correlation of vapor pressure data for high boiling hydrocarbons. *Ind. Eng. Chem.* **1955**, *47* (8), 1652–1658.

(35) Chang, J. S.; Lee, M. J.; Lin, H. M. Thermodynamic properties for model compounds of coal-liquids and their mixtures—Measurements and calculations. *Fluid Phase Equilib.* **2001**, *179* (1–2), 285–296.

(36) Evans, E. B. The viscosity of hydrocarbons. Parts VII and VIII. *J. Inst. Pet. Technol.* **1938**, *24*, 537.

(37) Tsierekzos, N. G.; Molinou, I. E.; Polizos, G. A. Relative permittivities, speeds of sound, viscosities, and densities of cyclohexanone plus *cis*-decalin and cyclohexanone plus *trans*-decalin mixtures at 283.15, 293.15, and 303.15 K. *J. Chem. Eng. Data* **2002**, *47* (6), 1492–1495.

(38) Ohnishi, K.; Fujihara, I.; Murakami, S. Thermodynamic properties of decalins mixed with hexane isomers at 298.15 K. 2. Excess volumes and isentropic compressibilities. *Fluid Phase Equilib.* **1989**, *46* (1), 73–84.

(39) McCullough, J. P.; Finke, H. L.; Messerly, J. F.; Todd, S. S.; Kincheloe, T. C.; Waddington, G. The low-temperature thermodynamic properties of naphthalene, 1-methylnaphthalene, 2-methylnaphthalene, 1,2,3,4-tetrahydro-naphthalene, *trans*-decahydronaphthalene and *cis*-decahydronaphthalene. *J. Phys. Chem.* **1957**, *61*, 1105–1116.

(40) Fenske, M. R.; Myers, H. S.; Quiggle, D. Normal decane–*trans*-decahydronaphthalene—Binary mixture for determining efficiencies of fractionating columns operating at reduced pressures. *Ind. Eng. Chem.* **1950**, *42* (4), 649–653.

(41) Mokbel, I.; Rauzy, E.; Loiseleur, H.; Berro, C.; Jose, J. Vapor pressures of 12 alkylcyclohexanes, cyclopentane, butylcyclopentane and *trans*-decahydronaphthalene down to 0.5 Pa. Experimental results, correlation and prediction by an equation of state. *Fluid Phase Equilib.* **1995**, *108*, 103–120.

(42) Sohda, M.; Iwai, Y.; Arai, Y.; Sakoguchi, A.; Ueoka, R.; Kato, Y. Vapor pressure of *cis*- and *trans*-decalins. *Netsu Sokutei* **1990**, *131*.

(43) Zeberg-Mikkelsen, C. K.; Baylaucq, A.; Barrouhou, M.; Boned, C. The effect of stereoisomerism on dynamic viscosity: A study of *cis*-decalin and *trans*-decalin versus pressure and temperature. *Phys. Chem. Chem. Phys.* **2003**, *5* (8), 1547–1551.

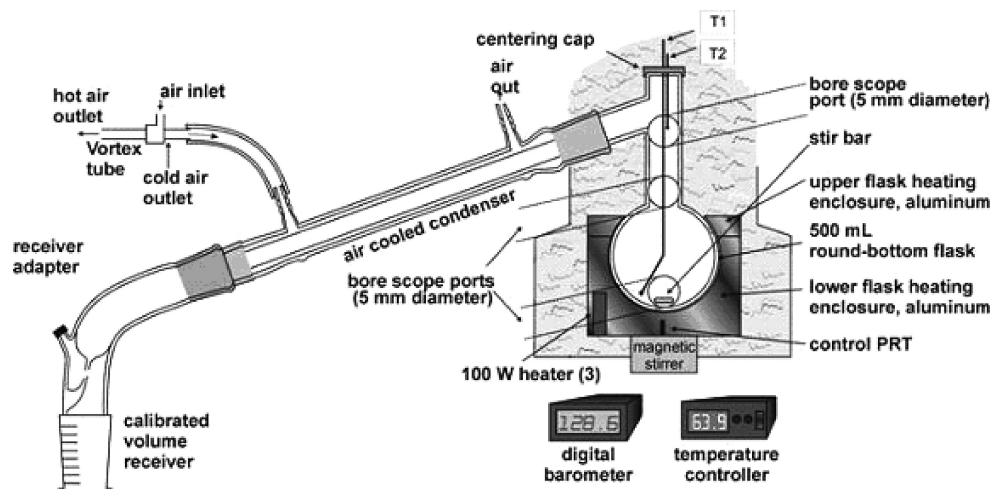


Figure 1. Schematic diagram of the overall apparatus used for the measurement of distillation curves.

Table 3. Distillation Curve for CDF at a Constant Atmospheric Pressure of 83.86 kPa^a

volume fraction	kettle temperature, T_k (K) at $p = 83.86$ kPa	kettle temperature, T_k (K) adjusted to 101.325 kPa with Sydney Young equation ^{95,96}
0.05	466.9	473.5
0.10	468.0	474.6
0.15	469.0	475.7
0.20	470.5	477.2
0.25	471.6	478.3
0.30	473.2	479.9
0.35	474.4	481.1
0.40	476.0	482.8
0.45	477.8	484.6
0.50	479.8	486.6
0.55	482.3	489.1
0.60	484.8	491.7
0.65	488.0	494.9
0.70	491.8	498.8
0.75	496.2	503.2
0.80	501.8	508.9
0.85	508.2	515.4
0.90	516.6	523.9

^a A detailed discussion of the uncertainty in these data is provided in ref 5.

Table 4. Composition of the Surrogate Mixture for the CDF

fluid	mole fraction
<i>n</i> -propylcyclohexane	0.04
<i>trans</i> -decalin	0.31
α -methyldecalin	0.28
bicyclohexyl	0.36
<i>n</i> -hexadecane	0.01

are represented to within 0.5%, as are the data of Ball and Trusler⁴⁸ for pressures up to 30 MPa. Deviations for the sound speed data of Ball and Trusler⁴⁸ increase systematically from 0.5% at 30 MPa to 3.0% at 100 MPa. Limited range (295–320 K) heat capacity at saturation pressure⁴⁹ are represented to within 1.5%; the liquid phase heat capacity measurements at pressures up to 10 MPa of Banipal et al.⁵⁰ are within 2%. Saturated liquid densities^{50–52} are represented to within 0.3%; liquid densities^{50,52–57} to 100 MPa are represented to within 0.4%. The vapor-pressure

(44) Hogenboon, D.; Webb, W.; Dixon, J. A. Viscosity of several liquid hydrocarbons as a function of temperature pressure and free volume. *J. Chem. Phys.* **1967**, *46* (7), 2586.

(45) Kuss, E.; Taslimi, M. *p*, *V*, *T* measurements on twenty organic liquids. *Chem. Ing. Tech.* **1970**, *42*, 1073–1081.

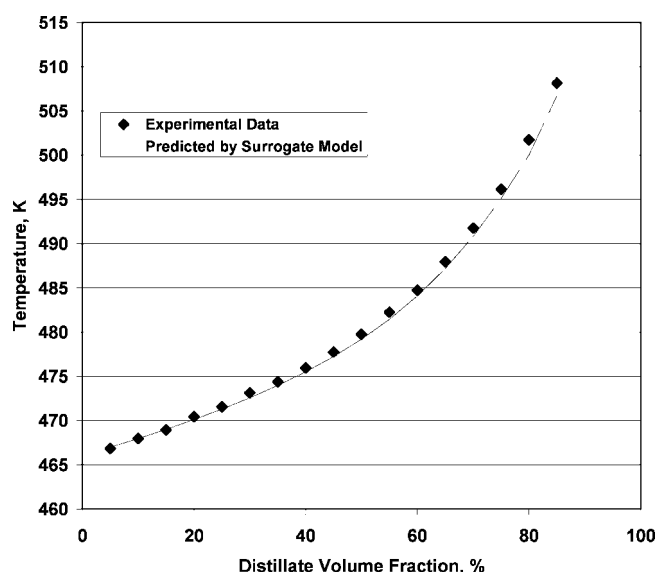


Figure 2. Experimental and calculated distillation curves for a CDF at 83.86 kPa.

Table 5. Selected Thermophysical Properties of a CDF

	temperature (K)	pressure (kPa)	density (g/mL)	sound speed (m/s)	viscosity (mPa s)
experimental value ⁵	293.15	83.86	0.8652	1385	2.3075
	298.15	83.86	0.8616	1365	2.1001
	303.15	83.86	0.8581	1349	1.9209
surrogate model	293.15	83.86	0.8718	1337	2.4214
	298.15	83.86	0.8680	1319	2.1972
	303.15	83.86	0.8642	1300	2.0037

data of Camin et al.⁵⁸ covering 463–559 K and the data of Morgan and Kobayashi⁵⁹ covering 393–583 K are represented to within 0.5%. On the basis of comparisons to the liquid phase viscosity data sets^{36,60–64} for pressures up to 100 MPa, we estimate that the uncertainty is 5%.

***n*-Hexylcyclohexane.** There are extremely limited experimental data for this fluid, and the equation of state was developed with predicted data generated by the TDE program.^{6,13} Comparisons show agreement to within 0.3% for the very limited atmospheric pressure liquid data that cover 293–298 K from refs 65–67. Vapor pressure data from Mokbel et al.⁴¹ show agreement to within 1% for temperatures from 340 to 467 K, with deviations of as much as 4% at lower temperatures. The normal boiling point predicted by the equation of state, 498.22 K, agrees to within the experimental uncertainty with

the value of 497.89 ± 1 K found by Mears et al.⁶⁵ Experimental viscosity data were unavailable; therefore, a predictive method, estimated to have an uncertainty of 15% in the liquid phase, was used.

α -Methyldecalin. There were extremely limited data for α -methyldecalin, and the equation of state was developed with predicted data generated by the TDE program.^{6,13} The equation predicts a normal boiling point of 479.89 K, which is in good agreement with a single experimental normal boiling point⁶⁸ of 478.11 K. Comparisons show agreement to within 0.8% for two density data at atmospheric pressure.^{68,69} Heat capacity measurements at saturation^{69,70} for the temperature range 311–423 K agree with values from the EOS to within 2%. On the basis of extremely limited experimental viscosity data,^{69,70} we estimate uncertainty in the liquid phase of 15%.

2,6-Dimethyldecalin. This fluid also had very limited experimental data: only a single liquid density and a normal boiling point. The EOS predicts a normal boiling point of 480.86 K that compares favorably to the experimental value of 481.11 K.⁶⁸ For a single liquid density at 293.145 K, the EOS predicts 867.5 kg/m³ and the experimental value⁶⁸ is 871 kg/m³. Experimental viscosity data were unavailable; therefore, a predictive method, estimated to have an uncertainty of 15% in the liquid phase, was used.

cis-Decalin. The speed of sound data^{37,38} are represented to

(46) Seyer, W. F.; Leslie, J. D. The viscosity of *cis* and *trans* decahydronaphthalene. *J. Am. Chem. Soc.* **1942**, *64*, 1912–1916.

(47) Bolotnikov, M. F.; Neruchev, Y. A.; Melikhov, Y. F.; Verveiko, V. N.; Verveiko, M. V. Temperature dependence of the speed of sound, densities, and isentropic compressibilities of hexane plus hexadecane in the range of (293.15 to 373.15) K. *J. Chem. Eng. Data* **2005**, *50* (3), 1095–1098.

(48) Ball, S. J.; Trusler, J. P. M. Speed of sound of *n*-hexane and *n*-hexadecane at temperatures between 298 and 373 K and pressures up to 100 MPa. *Int. J. Thermophys.* **2001**, *22* (2), 427–443.

(49) Finke, H. L.; Gross, M. E.; Waddington, G.; Huffman, H. M. Low-temperature thermal data for the 9 normal paraffin hydrocarbons from octane to hexadecane. *J. Am. Chem. Soc.* **1954**, *76* (2), 333–341.

(50) Banipal, T. S.; Garg, S. K.; Ahluwalia, J. C. Heat capacities and densities of liquid normal octane, normal nonane, normal decane, and normal hexadecane at temperatures from 318.15 K to 373.15 K and at pressures up to 10 MPa. *J. Chem. Thermodyn.* **1991**, *23* (10), 923–931.

(51) Dymond, J. H.; Young, K. J. Transport properties of nonelectrolyte liquid mixtures—I. Viscosity coefficients for *n*-alkane mixtures at saturation pressure from 283 to 378 K. *Int. J. Thermophys.* **1980**, *1* (4), 331–344.

(52) Dymond, J. H.; Harris, K. R. The temperature and density dependence of the self-diffusion coefficient of normal hexadecane. *Mol. Phys.* **1992**, *75* (2), 461–466.

(53) Snyder, P. S.; Winnick, J. The pressure, volume and temperature properties of liquid *n*-alkanes at elevated pressures. *Proc. Symp. Thermophys. Prop.* **1970**, *5*, 115–29.

(54) Gouel, P. Specific volume of cycloalkanes and alkylbenzenes (C6–C16). *Bull. Cent. Rech. Elf Explor. Prod.* **1978**, *2*, 211–225.

(55) Glaser, M.; Peters, C. J.; Vanderkooi, H. J.; Lichtenthaler, R. N. Phase equilibria of (methane + *n*-hexadecane) and (*P*, *V*_m, *T*) of *n*-hexadecane. *J. Chem. Thermodyn.* **1985**, *17* (9), 803–815.

(56) Chang, J. S.; Lee, M. J.; Lin, H. M. Densities of binary mixtures of hexadecane with *m*-xylene and tetralin from 333 to 413 K and pressures up to 30 MPa. *J. Chem. Eng. Data* **1998**, *43* (2), 233–237.

(57) Amorim, J. A.; Chiavone-Filho, O.; Paredes, M. L. L.; Rajagopal, K. High-pressure density measurements for the binary system cyclohexane plus *n*-hexadecane in the temperature range of (318.15 to 413.15) K. *J. Chem. Eng. Data* **2007**, *52* (2), 613–618.

(58) Camin, D. L.; Forziati, A. F.; Rossini, F. D. Physical properties of *n*-hexadecane, *n*-decylcyclopentane, *n*-decylcyclohexane, 1-hexadecene and *n*-decylbenzene. *J. Phys. Chem.* **1954**, *58*, 440–442.

(59) Morgan, D. L.; Kobayashi, R. Direct vapor-pressure measurements of 10 *n*-alkanes in the C-10–C(28) range. *Fluid Phase Equilib.* **1994**, *97*, 211–242.

(60) Golubev, I. F. *Viscosity of Gases and Gas Mixtures. A Handbook*; Israel Program for Scientific Translations: Jerusalem, Israel, 1970; p 245.

(61) Ducoulombier, D.; Zhou, H.; Boned, C.; Peyrelasse, J.; Saint-Guirons, H.; Xans, P. Pressure (1–1000 bar) and temperature (20–100 °C) dependence of the viscosity of liquid hydrocarbons. *J. Phys. Chem.* **1986**, *90*, 1692–1700.

within 2%; the heat capacity at saturation data of McCullough³⁹ are represented to within 3% at 350 K, increasing to 6% at 230 K; while the data of Gudzinowicz⁶⁹ over 313–423 K are within 2%. Deviations in vapor pressure^{40,42,71} are generally within 2%; saturated liquid densities^{37,43,44} are within 0.1%; and the density values^{43,44,72} as a function of pressures less than 100 MPa are within 1%. On the basis of comparisons to the data of Zeberg-Mikkelsen et al.⁴³ that cover 293–353 K at pressures to 100 MPa and the data of Seyer and Leslie,⁴⁶ we estimate the uncertainty of the viscosity in the liquid phase to be less than 8%.

Mixture Properties

For calculations of the thermodynamic properties of mixtures, we use a mixture model explicit in Helmholtz energy that can use any equation of state, provided that it can be expressed in terms of the Helmholtz energy.⁷³ This form of model has been used successfully for refrigerant mixtures⁷³ and natural gas mixtures.⁷⁴ Details on the mixture model are given in refs 73 and 75

The model for calculating the transport properties of a mixture is an extended corresponding states method.^{23,27,76–79} The basic procedure is based on the earlier work of Ely and Hanley.^{80,81} In this approach, the viscosity or thermal conductivity of a mixture is calculated in a two-step procedure. First, mixing and combining rules are used to represent the mixture in terms of a hypothetical pure fluid, and then the properties of the hypothetical pure fluid are determined by mapping onto a reference fluid through the use of “shape factors”; details are given elsewhere.^{23,27,76–79} For both refrigerant mixtures and mixtures of natural gas components, the viscosity and thermal conductivity are typically represented to within 5–10%,⁷⁶ except for the viscosity of fluids near freezing and the thermal conductivity near the critical point, where errors can be larger. We expect similar results with the mixtures in this work because they are primarily nonpolar hydrocarbons.

The distillation curve of complex multicomponent fluids has traditionally been used to describe fluid volatility, usually by application of the metrology described in ASTM D-86.⁸² The distillation curve is a graphical depiction of the boiling

(62) Dymond, J. H.; Young, K. J.; Isdale, J. D. Transport properties of nonelectrolyte liquid mixtures—II. Viscosity coefficients for the *n*-hexane + *n*-hexadecane system at temperatures from 25 to 100 °C at pressures up to the freezing pressure or 500 MPa. *Int. J. Thermophys.* **1980**, *1* (4), 345–373.

(63) Dymond, J. H.; Young, K. J. Transport properties of nonelectrolyte liquid mixtures—V. Viscosity coefficients for binary mixtures of benzene plus alkanes at saturation pressure from 283 to 393 K. *Int. J. Thermophys.* **1981**, *2* (3), 237–247.

(64) Queimada, A. J.; Quinones-Cisneros, S. E.; Marrucho, I. M.; Coutinho, J. A. P.; Stenby, E. H. Viscosity and liquid density of asymmetric hydrocarbon mixtures. *Int. J. Thermophys.* **2003**, *24* (5), 1221–1239.

(65) Mears, T. W.; Stanley, C. L.; Compere, E. L.; Howard, F. L. Synthesis, purification, and physical properties of seven twelve-carbon hydrocarbons. *J. Res. Natl. Bur. Stand., A* **1963**, *67*, 475.

(66) Bourguet, M. *Bull. Soc. Chim. France* **1927**, *41*, 1475.

(67) Schlenk, W. *Justus Liebig's Ann. Chem.* **1951**, *573*, 142–162.

(68) Weissenberger, G.; Henke, R.; Katschinka, H. Binary liquid mixtures. XX. Systems with substituting hydronaphthalenes. *Z. Anorg. Allg. Chem.* **1926**, *153*, 33.

(69) Gudzinowicz, B. J.; Campbell, R. H.; Adams, J. S. Specific heat measurements of complex saturated hydrocarbons. *J. Chem. Eng. Data* **1963**, *8* (2), 201–204.

(70) Gollis, M. H.; Belenyessy, L. I.; Gudzinowicz, B. J.; Koch, S. D.; Smith, J. O.; Wineman, R. J. Evaluation of pure hydrocarbons as jet fuels. *J. Chem. Eng. Data* **1962**, *7*, 311–316.

(71) Gupta, A.; Gupta, S.; Groves, F. R.; McLaughlin, E. Measurement of vapor–liquid equilibrium for binary systems containing polynuclear aromatic compounds. *Fluid Phase Equilib.* **1991**, *65*, 305–326.

temperature of the fluid plotted against volume or volume fraction. Unfortunately, the classical application of this distillation curve measurement method, while standardized, has no basis in theory and cannot be used to represent thermodynamic state points. To remedy this problem, an advanced distillation curve metrology has been developed.^{5,83–94} This new method is a significant improvement over current approaches, featuring (1) a composition explicit data channel for each distillate fraction (for both qualitative and quantitative analysis), (2) temperature measurements that are true thermodynamic state points that can be modeled with an equation of state, (3) temperature, volume, and pressure measurements of low uncertainty suitable for equation of state development, (4) consistency with a century of historical data, (5) an assessment of the energy content of each distillate fraction, (6) trace chemical analysis of each distillate fraction, and (7) corrosivity assessment of each distillate fraction. The apparatus for this metrology is illustrated schematically in Figure 1. As pointed out in earlier work,⁸³ the specific location of the thermocouple in the liquid in the boiling flask or kettle, T1 in Figure 1, allows the process to be modeled, because it represents a thermodynamic state point, is easily reproducible, and is preferable to the head temperature, which is very sensitive to placement in the apparatus as well as the heating rate.⁸³ The data for the distillation curve for the CDF in this work are given in Table 3 and include values adjusted to 101.325 kPa with the Sydney Young equation,^{95–97} as well as the raw data taken at the local atmospheric pressure of 83.86 kPa.

Following previous work,³ we modeled the distillation process as a simple batch distillation,^{98,99} where the vapor leaving the boiling flask and head passes into a total condenser without reflux. The liquid in the kettle is assumed to be heated to its bubble point, and it is assumed to be in equilibrium with its vapor phase. The vapor is subsequently removed at a constant flow rate. We note that the measurement is also performed at a constant mass flow rate through the distillation head, a feature accomplished with a model predictive temperature controller.¹⁰⁰

(72) Miyake, Y.; Baylaucq, A.; Zeberg-Mikkelsen, C. K.; Galliero, G.; Ushiki, H.; Boned, C. Stereoisomeric effects on volumetric properties under pressure for the system *cis*- plus *trans*-decalin. *Fluid Phase Equilib.* **2007**, 252 (1–2), 79–87.

(73) Lemmon, E. W.; Jacobsen, R. T. Equations of state for mixtures of R-32, R-125, R-134a, R-143a, and R-152a. *J. Phys. Chem. Ref. Data* **2004**, 33 (2), 593–620.

(74) Kunz, O.; Klimeck, R.; Wagner, W.; Jaeschke, M. *The GERG-2004 Wide-Range Reference Equation of State for Natural Gases and Other Mixtures*; GERG Technical Monograph; Fortsch.-Ber. VDI, VDI-Verlag: Dusseldorf, Germany, 2007.

(75) Lemmon, E. W.; McLinden, M. O. In Method for estimating mixture equation of state parameters, Thermophysical Properties and Transfer Processes of New Refrigerants Conference, International Institute of Refrigeration, Commission B1, Paderborn, Germany, 2001; pp 23–30.

(76) Chichester, J.; Huber, M. L. *Extended Corresponding States Model for Viscosity and Thermal Conductivity of Pure Fluids and Their Mixtures as Implemented in REFPROP Version 8*, NIST IR 6650; National Institute of Standards and Technology: Boulder, CO, 2007.

(77) McLinden, M. O.; Klein, S. A.; Perkins, R. A. An extended corresponding states model for the thermal conductivity of pure refrigerants and refrigerant mixtures. *Int. J. Refrig.* **2000**, 23 (1), 43–63.

(78) Klein, S. A.; McLinden, M. O.; Laesecke, A. An improved extended corresponding states method for estimation of viscosity of pure refrigerants and mixtures. *Int. J. Refrig.* **1997**, 20 (3), 208–217.

(79) Huber, M. L.; Ely, J. F. Prediction of the thermal conductivity of refrigerants and refrigerant mixtures. *Fluid Phase Equilib.* **1992**, 80, 249–261.

(80) Ely, J. F.; Hanley, H. J. M. Prediction of transport properties. 1. Viscosity of fluids and mixtures. *Ind. Eng. Chem. Fundam.* **1981**, 20 (4), 323–332.

(81) Ely, J. F.; Hanley, H. J. M. Prediction of transport properties. 2. Thermal conductivity of pure fluids and mixtures. *Ind. Eng. Chem. Fundam.* **1983**, 22 (1), 90–97.

The vapor–liquid equilibrium for the system is represented with the mixture model,^{74,101} described above with estimated interaction parameters,⁷⁵ and incorporates the pure fluid Helmholtz equations of state given in parts a–g of Table 2. We used these equations and mixing rules as implemented in the REFPROP computer program.¹⁰²

Results and Discussion

We used a regression procedure to minimize the differences between the experimental advanced distillation curve and the predictions of the model to determine the compositions of the surrogate fluid mixture. For the regression, we used the raw uncorrected values in Table 3. The objective function was the sum of the squared percentage differences between the experimental distillation curve data⁵ and the predicted value. Following previous work,³ the distillation curve was constructed from a series of bubble-point calculations, where the input for generation of a distillation curve is the initial composition of the sample in the distillation flask and the ambient pressure. Thus, for our regression procedure to determine the surrogate mixture, the independent variables are the compositions of the fluid mixture. Our initial guess included all of the components in Table 1. Successive calculations gave very small concentrations of some components. These were removed from the mixture, and the minimization process was repeated. The final surrogate composition, containing five components, is given in Table 4. The computed distillation curve (adjusted with a apparatus-specific volume shift of 0.12, described in ref 3) and the experimental data are shown in Figure 2. The difference between the calculated and experimental distillation temperatures is always within 2 K. The lightest (*n*-propylcyclohexane) and heaviest (*n*-hexadecane) fluids are present only in small amounts and determine the initial boiling behavior and the tail of the distillation curve. The remaining components determine the overall shape of the curve. Good agreement was found between the initial boiling point observed experimentally,⁵ 465.45 K, and the calculated initial boiling point (at 83.86 kPa) of 464.54 K.

(82) *Standard Test Method for Distillation of Petroleum Products at Atmospheric Pressure*, ASTM Standard D 86-04b; American Society for Testing and Materials: West Conshohocken, PA, 2004.

(83) Bruno, T. J. Improvements in the measurement of distillation curves. 1. A composition-explicit approach. *Ind. Eng. Chem. Res.* **2006**, 45, 4371–4380.

(84) Bruno, T. J.; Smith, B. L. Improvements in the measurement of distillation curves. 2. Application to aerospace/aviation fuels RP-1 and S-8. *Ind. Eng. Chem. Res.* **2006**, 45, 4381–4388.

(85) Bruno, T. J. Method and apparatus for precision in-line sampling of distillate. *Sep. Sci. Technol.* **2006**, 41 (2), 309–314.

(86) Bruno, T. J.; Smith, B. L. Enthalpy of combustion of fuels as a function of distillate cut: Application of an advanced distillation curve method. *Energy Fuels* **2006**, 20 (5), 2109–2116.

(87) Smith, B. L.; Bruno, T. J. Advanced distillation curve measurement with a model predictive temperature controller. *Int. J. Thermophys.* **2006**, 27 (5), 1419–1434.

(88) Smith, B. L.; Bruno, T. J. Improvements in the measurement of distillation curves. 3. Application to gasoline and gasoline plus methanol mixtures. *Ind. Eng. Chem. Res.* **2007**, 46 (1), 297–309.

(89) Smith, B. L.; Bruno, T. J. Improvements in the measurement of distillation curves. 4. Application to the aviation turbine fuel jet-A. *Ind. Eng. Chem. Res.* **2007**, 46 (1), 310–320.

(90) Smith, B. L.; Bruno, T. J. Application of a composition-explicit distillation curve metrology to mixtures of jet-A + synthetic Fischer–Tropsch S-8. *J. Propul. Power* **2008**, 24 (3), 619–623.

(91) Ott, L. S.; Bruno, T. J. Corrosivity of fluids as a function of distillate cut: Application of an advanced distillation curve method. *Energy Fuels* **2007**, 21, 2778–2784.

(92) Ott, L. S.; Bruno, T. J. Modifications to the copper strip corrosion test for the measurement of microscale samples. *J. Sulfur Chem.* **2007**, 28 (5), 493–504.

Limited experimental data are available⁵ for the sound speed, density, and viscosity of the CDF; therefore, we can evaluate the performance of the surrogate mixture with the actual fuel properties. Results are shown in Table 5. The predicted and experimental values of density, sound speed, and viscosity are within 1, 4, and 5%, respectively. To represent the distillation curve, it is necessary to use a mixture model. However, if one is interested only in single-phase properties, pure *trans*-decalin can be used to model the density, sound speed, and viscosity to within 1, 1, and 8%, respectively. Note that, if one uses pure

cis-decalin, the results are much less satisfactory with deviations of 4, 4, and 50%. The experimental data are at atmospheric pressure and cover a very small temperature range, and we expect deviations to be larger outside this region, with the largest deviations expected for the viscosity at low temperatures and high pressures; however, these results are encouraging for a predictive model.

Conclusions

In this paper, we have presented a five-component surrogate mixture model for representation of the thermophysical properties of a synthetic coal-derived aviation fuel. A key feature is the use of experimental data from the advanced distillation curve metrology that permits modeling the volatility behavior of the surrogate mixture. The procedure for correlating and incorporating the distillation-curve data is general and may be applied to develop other surrogate fuel mixtures. The surrogate model, developed only with the data from the distillation curve, was then used to predict the density, sound speed, and viscosity of the CDF mixture and found to give deviations of 1, 4, and 5%, respectively. Future work will use this process to determine surrogate models for other complex fuels.

Acknowledgment. We gratefully acknowledge the financial support of the NASA/Glenn Research Center under agreement NNC08IA04I and the Air Force Research Laboratory Propulsion Directorate, Wright Patterson Air Force Base, MIPRF4FBY6346G001. We also acknowledge our NIST colleagues Dr. A. Laesecke, Dr. R. Perkins, S. Outcalt, and Dr. M. McLinden for helpful discussions and sharing their data prior to publication.

EF800314B

(93) Ott, L. S.; Smith, B. L.; Bruno, T. J. Advanced distillation curve measurements for corrosive fluids: Application to two crude oils. *Fuel* **2008**, in press.

(94) Ott, L. S.; Smith, B. L.; Bruno, T. J. Advanced distillation curve measurement: Application to a bio-derived crude oil prepared from swine manure. *Fuel* **2008**, in press.

(95) Young, S. Correction of boiling points of liquids from observed to normal pressures. *Proc. Chem. Soc.* **1902**, 81, 777.

(96) Young, S. *Fractional Distillation*; Macmillan and Co, Ltd.: London, U.K., 1903.

(97) Ott, L. S.; Smith, B. L.; Bruno, T. J. Experimental test of the Sydney Young equation for the presentation of distillation curves. *J. Chem. Thermodynam.* **2008**, in press.

(98) Kister, H. Z. *Distillation Design*; McGraw-Hill, Inc.: New York, 1992.

(99) Geankoplis, C. J. *Transport Processes and Unit Operations*, 3rd ed.; Prentice Hall: Englewood Cliffs, NJ, 1993.

(100) Smith, B. L.; Bruno, T. J. Advanced distillation curve measurement with a model predictive temperature controller. *Int. J. Thermophys.* **2006**, 27, 1419–1434.

(101) Lemmon, E. W.; Jacobsen, R. T. A generalized thermodynamic model for the thermodynamic properties of mixtures. *Int. J. Thermophys.* **1999**, 20 (3), 825–835.

(102) Lemmon, E. W.; Huber, M. L.; McLinden, M. O. *NIST Standard Reference Database 23, NIST Reference Fluid Thermodynamic and Transport Properties Database (REFPROP): Version 8.0*, Standard Reference Data, National Institute of Standards and Technology: Gaithersburg, MD, 2007.